Electronic Supplementary Information

Controlling lability of uranyl(VI) through intramolecular π-π stacking

Takanori Mashita,[a] Satoru Tsushima[b,c], Koichiro Takao[a]*

[a] Laboratory for Advanced Nuclear Energy, Tokyo Institute of Technology 2-12-1-N1-32, O-okayama, Meguro-ku, 152-8550 Tokyo, Japan

[b] Tokyo Tech World Research Hub Initiative (WRHI), Institute of Innovative Research, Tokyo Institute of Technology, 2-12-1, O-okayama, Meguro-ku, 152-8550 Tokyo, Japan

[b] Institute of Resource Ecology, Helmholtz-Zentrum Dresden-Rossendorf e.V.Bautzner Landstraße 400, 01328 Dresden, Germany

Table S1 Activation Parameters and Kinetic Data of Ligand Exchange Reactions of Different UO_2^{2+} Complexes with CN = 4, 5

L (solvent)	CN	mechanism	$\Delta H^{\ddagger}$ [a] $\Delta S^{\ddagger}$ [b]	$\Delta G^{\ddagger}_{298}$ [c]	k^{298} [d]	ref.
					(k_D /s^{-1})	
$OPCyPh_2$ (CD_3NO_2)	4	A	6.9 ± 1.0 −174 ± 3	58.8	3.1×10^2	this work
$OPPh_3$ (CD_2Cl_2)	4	A	7.1 ± 0.3 −122 ± 1	43.5	1.4×10^5	S1
HMPA (CD_2Cl_2)	4	A	22.2 ± 3 −120 ± 9	58.0	4.3×10^2	S2
					(k_A /$M^{-1}\cdot s^{-1}$)	
$OPCyPh_2$ (CD_3NO_2)	4	D	6.6 ± 1.0 −202 ± 3	66.9	12	this work
HMPA (CD_2Cl_2)	4	D	14 ± 3 −172 ± 11	65.3	23	S2
$UO_2(DMA)_5^{2+}$	5	D	42.6 ± 0.2 −43.5 ± 0.7	55.6	1.1×10^3	S3
$UO_2(H_2O)_5^{2+}$	5	D	28.4 ± 1 −31 ± 3	37.6	1.6×10^6	S4
$UO_2(acac)_2DMSO$	5	D	45.8 ± 0.8 −46.6 ± 2.9	59.7	2.1×10^2	S5
$UO_2(acac)_2DMSO$	5	D	47.9 ± 5.2 −46.6 ± 11.2	61.8	92	S5
$UO_2(acac)_2DMF$	5	D	42 ± 1.3 −46.2 ± 5.5	55.8	1.0×10^3	S5
$UO_2(acac)_2DMF$	5	D	32.8 ± 1.7 −92 ± 5.9	60.2	1.7×10^2	S5
$UO_2(salophen)_2DMSO$	5	D	30 ± 1 −84 ± 1	55.0	1.4×10^3	S6
$UO_2(salophen)_2DMF$	5	D	28 ± 1 −89 ± 4	54.5	1.7×10^3	S6

[a] Activation enthalpy in $kJ\cdot mol^{-1}$. [b] Activation entropy in $J\cdot mol^{-1}\cdot K^{-1}$. [c] Gibbs free energy for activation at 298 K in $kJ\cdot mol^{-1}$. [d] Rate constant at 298 K.

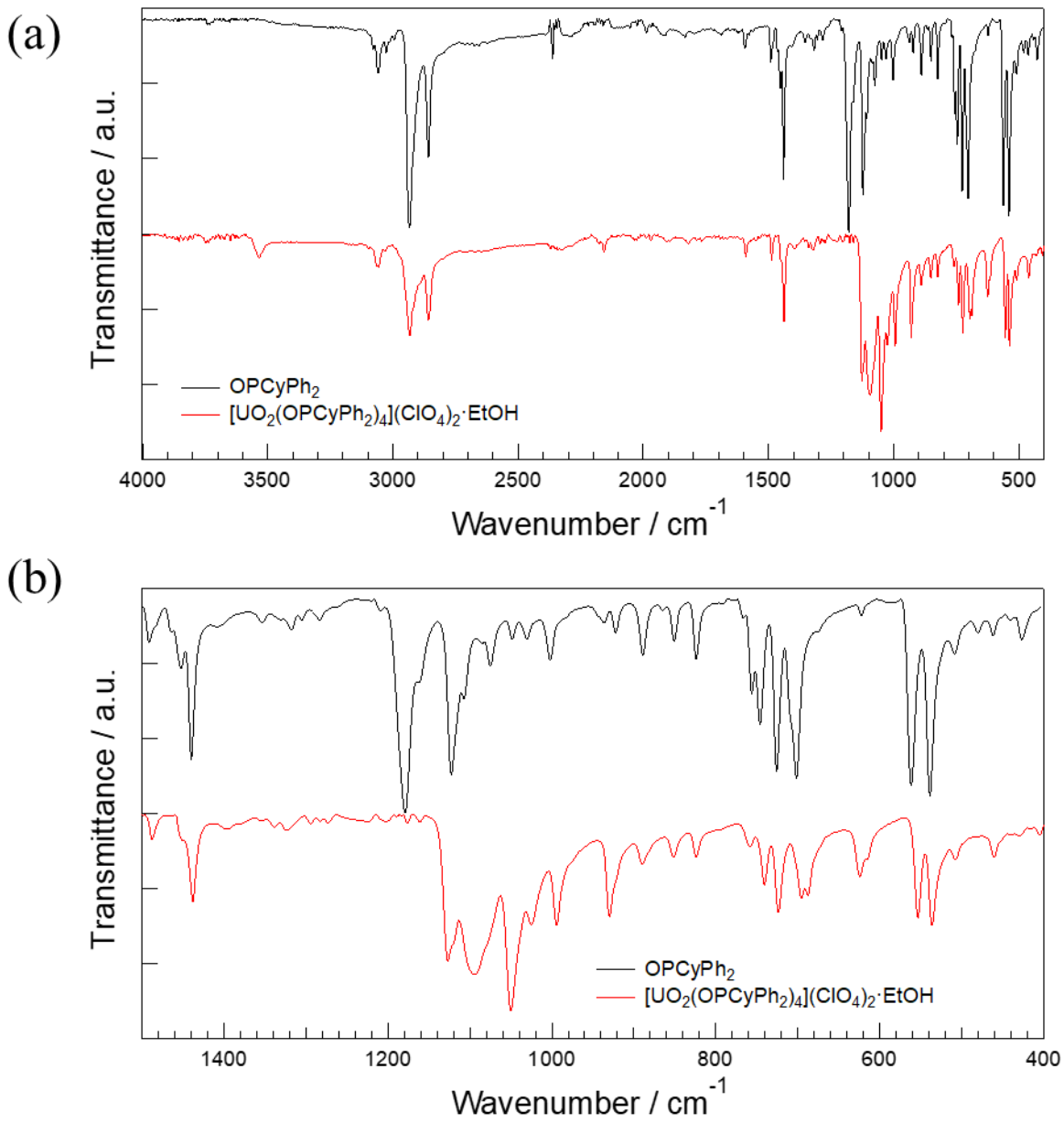

Fig. S1. IR spectra of $OPCyPh_2$ (black), and $[UO_2(OPCyPh_2)_4](ClO_4)_2 \cdot EtOH$ (red). Wavenumber range: (a) 4000 ~ 400 cm^{-1}, (b) 1500 ~ 400 cm^{-1}.

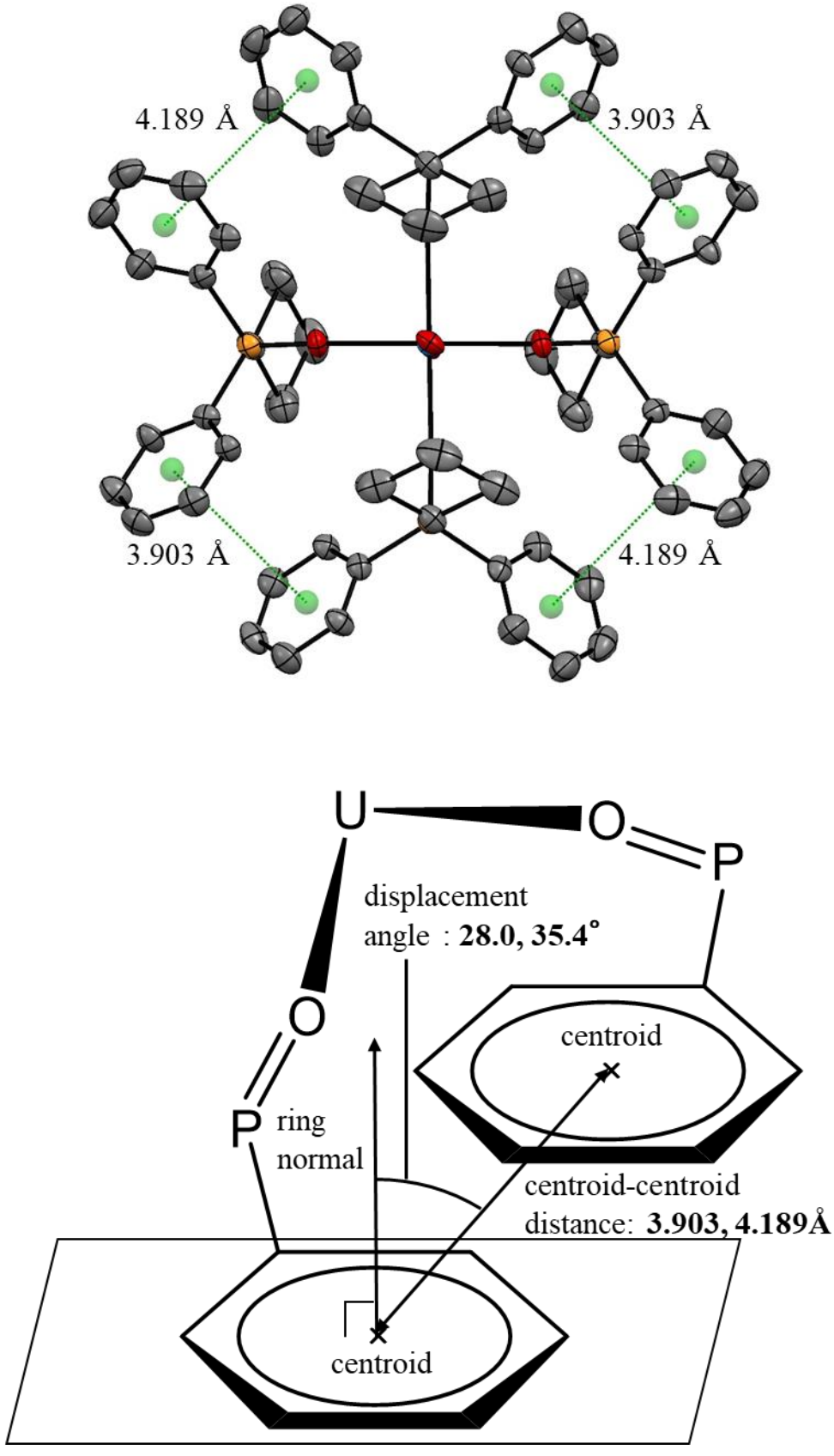

Fig. S2. Top view of molecular structure (top) and schematic drawing of intramolecular π–π stacking interactions (bottom) of $[UO_2(OPCyPh_2)_4]^{2+}$.

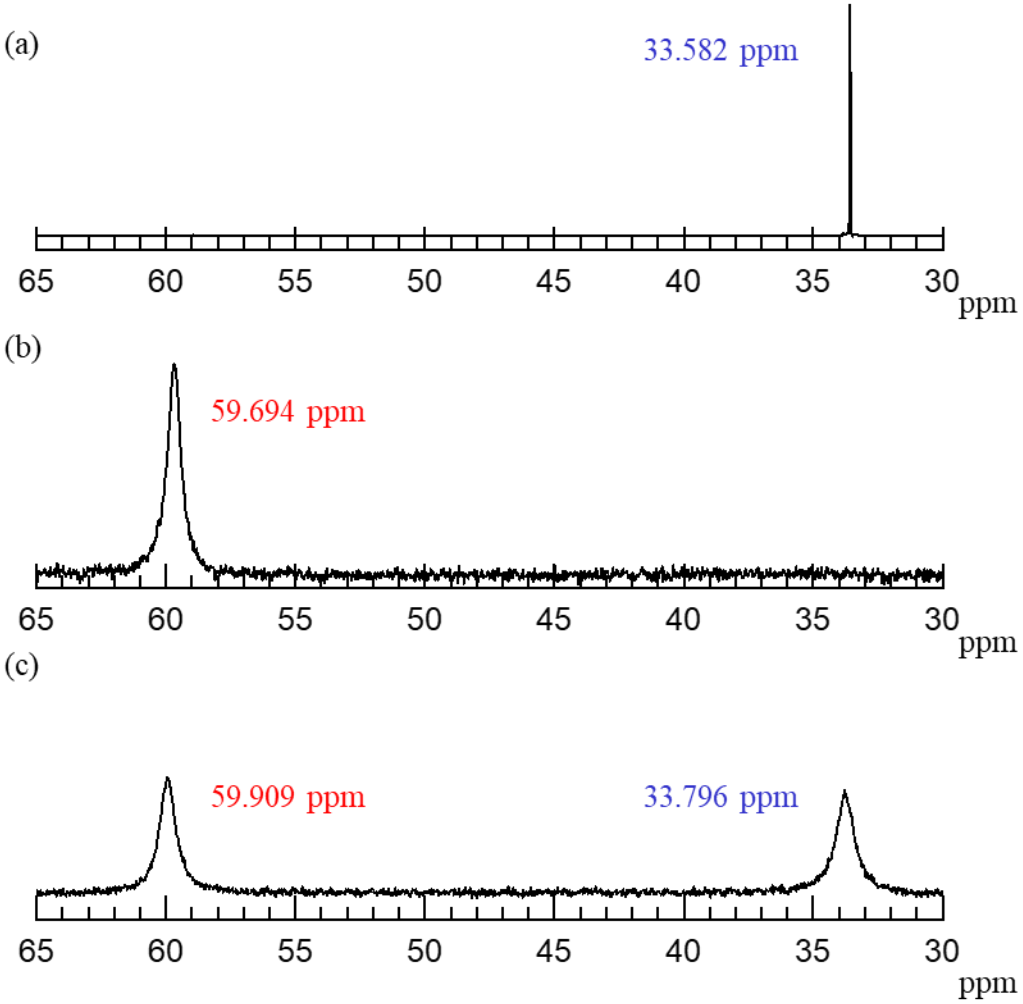

Fig. S3. $^{31}P\{^{1}H\}$ NMR spectra of CD_2Cl_2 solutions dissolving (a) $OPCyPh_2$, (b) $[UO_2(OPCyPh_2)_4](ClO_4)_2 \cdot EtOH$, (c) $OPCyPh_2$ and $[UO_2(OPCyPh_2)_4](ClO_4)_2 \cdot EtOH$ at 298K.

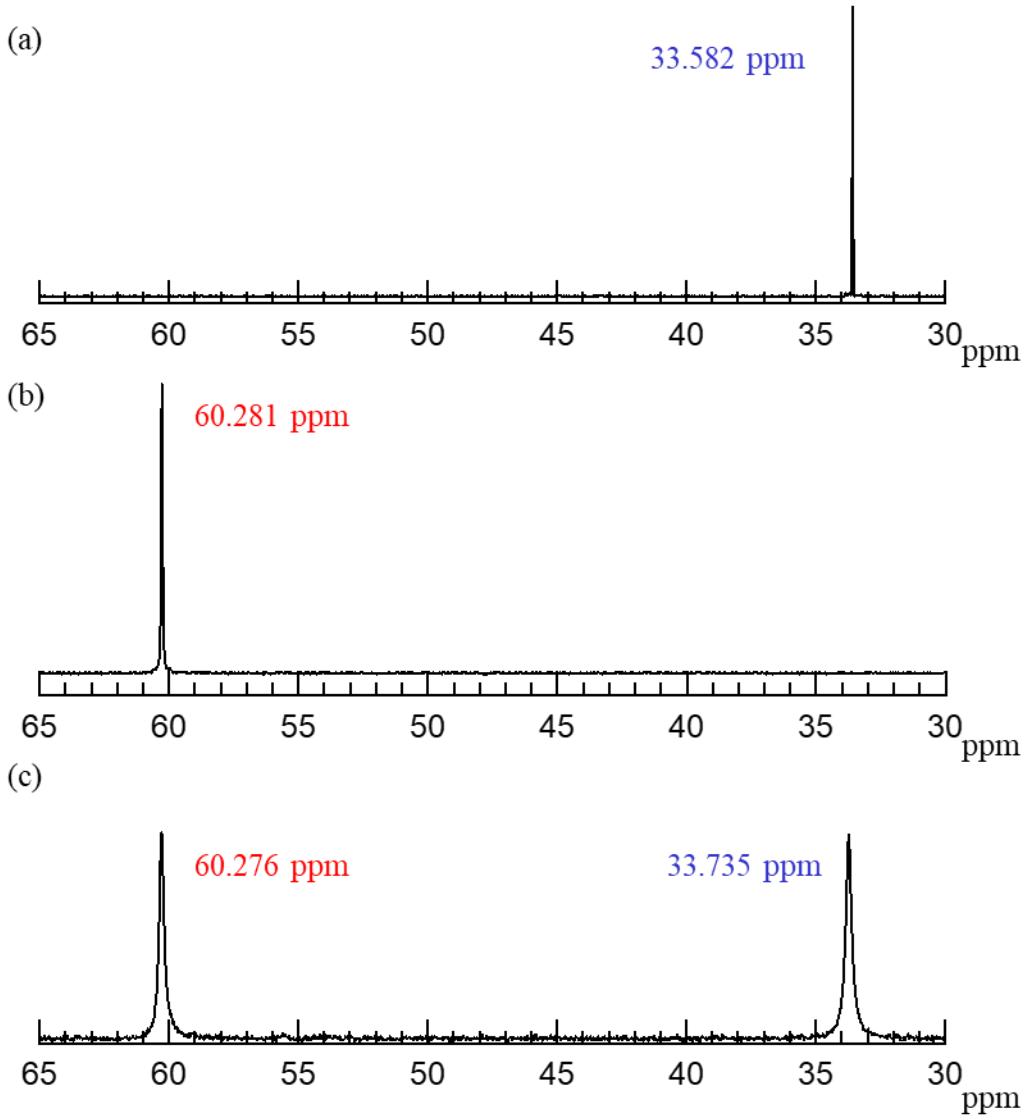

Fig. S4. $^{31}P\{^{1}H\}$ NMR spectra of CD_3NO_2 solutions dissolving (a) $OPCyPh_2$, (b) $[UO_2(OPCyPh_2)_4](ClO_4)_2 \cdot EtOH$, (c) $OPCyPh_2$ and $[UO_2(OPCyPh_2)_4](ClO_4)_2 \cdot EtOH$ at 298K.

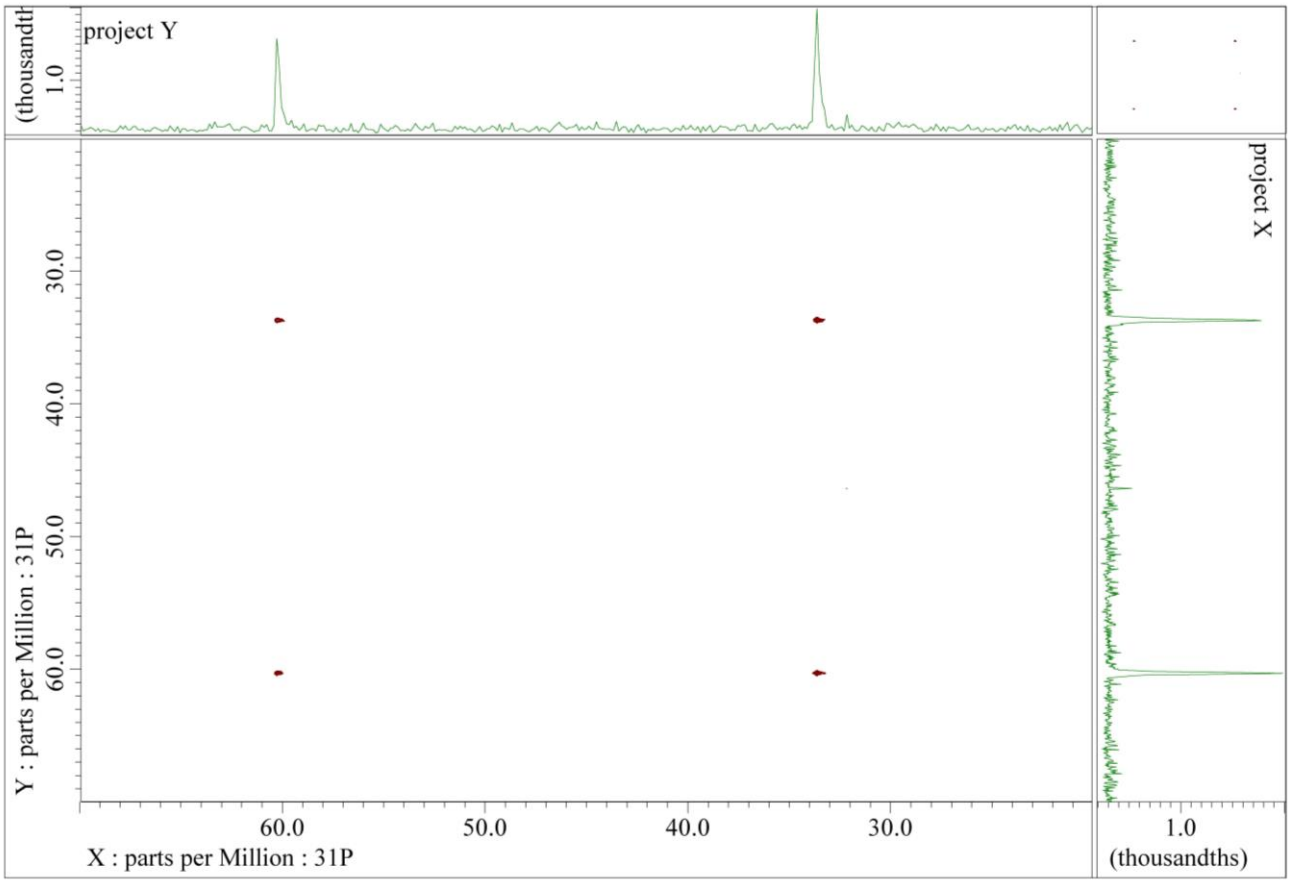

Fig. S5. 2D $^{31}P\{^{1}H\}$ EXSY NMR spectra of CD_3NO_2 solution dissolving $OPCyPh_2$ (39.69 mM) and $[UO_2(OPCyPh_2)_4](ClO_4)_2 \cdot EtOH$ (9.98 mM).

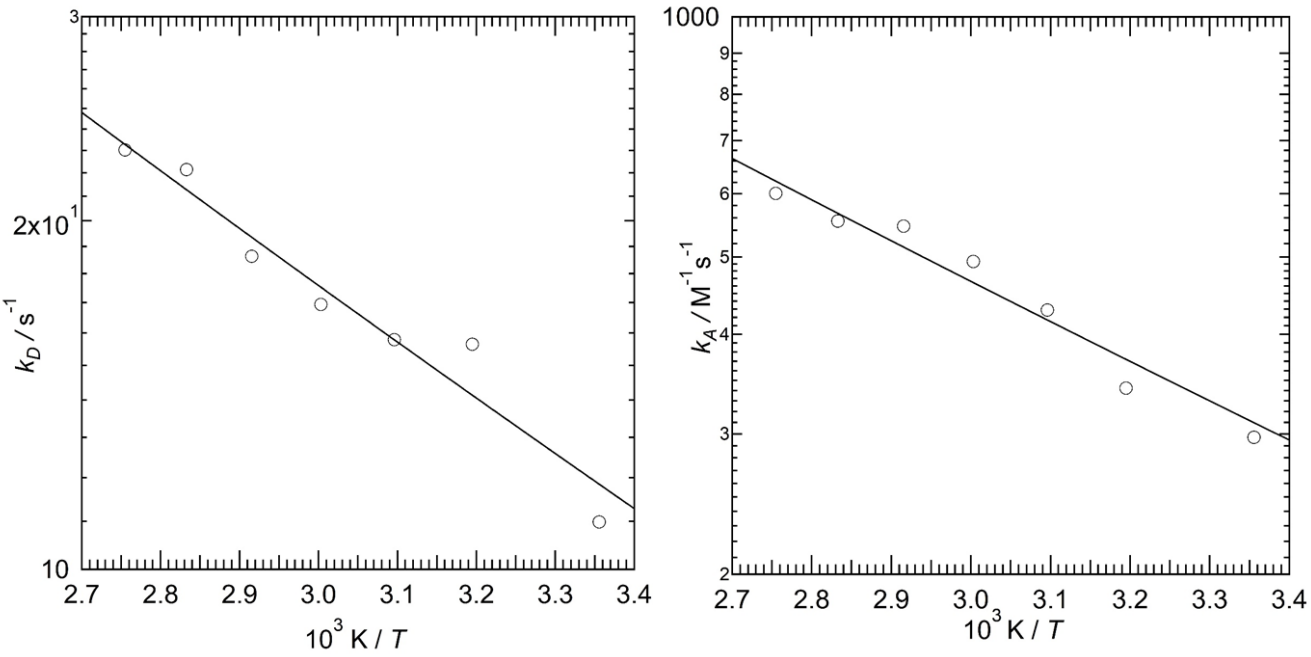

Fig. S6. Eyring plots for (a) k_D and (b) k_A.

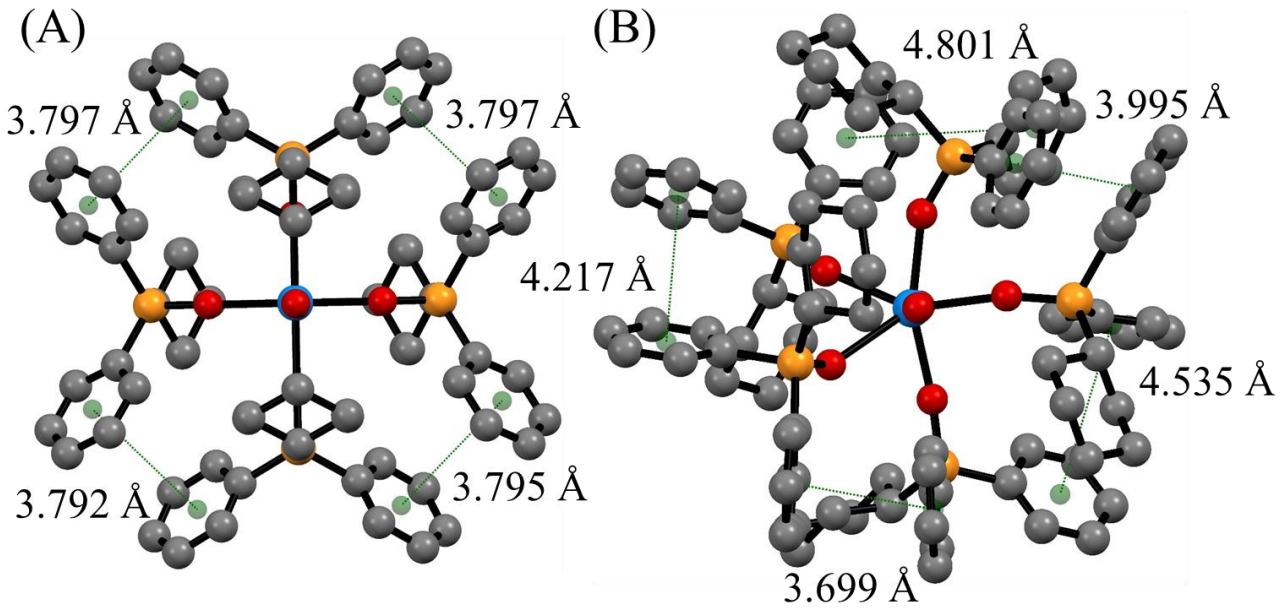

Fig. S7. Optimized structures of $[UO_2(OPCyPh_2)_4]^{2+}$ (panel A) and $[UO_2(OPCyPh_2)_5]^{2+}$ (panel B) at CAM-B3LYP-D3 level in the top views along axial UO_2^{2+} moieties. Distances between centroids (green dots) of the phenyl groups involved in the π–π stacking interactions are also displayed.

References.

S1. K. Takao, T. Takahashi and Y. Ikeda, *Inorg. Chem.*, 2009, **48**, 1744-1752.
S2. G. J. Honan, S. F. Lincoln and E. H. Williams, *Inorg. Chem.*, 1978, **17**, 1855-1857.
S3. R. P. Bowen, S. F. Lincoln and E. H. Williams, *Inorg. Chem.*, 1976, **15**, 2126-2129.
S4. I. Farkas, I. Bányai, Z. Szabó, U. Wahlgren and I. Grenthe, *Inorg. Chem.*, 2000, **39**, 799-805.
S5. Y. Ikeda, H. Tomiyasu and H. Fukutomi, *Inorg. Chem.*, 1984, **23**, 1356-1360.
S6. K. Takao and Y. Ikeda, *Inorg. Chem.*, 2007, **46**, 1550-1562.